

Modeling Laser-Generated Cavitation Bubbles

C.M. Christian¹, E.G. Paterson² and A.A. Fontaine¹

¹Applied Research Laboratory
The Pennsylvania State University, State College, PA 16804 U.S.A.

²Department of Aerospace and Ocean Engineering
Virginia Polytechnic Institute and State University, Blacksburg, VA 24061

Abstract

Cavitation in turbomachinery can impact performance and lifecycle. The formation and collapse of cavitating bubbles near a surface releases significant energy in a very short time often resulting in erosion damage. Considerable research has focused on understanding the physics of bubble formation and collapse, and how this collapse relates to surface erosion. To date this has been an elusive goal due to the process physics, flow and temporal scales and experimental and computational limitations. This research focused on developing a computational model of cavitation bubble formation and collapse to be used to develop erosion prediction tools. The dynamics associated with the formation of a laser-pulse generated bubble and its collapse against a solid wall was computationally modeled with OpenFOAM using a compressible multi-phase pressure-based solver. A conservation of energy model was developed to predict the localized heating occurring at the focal point of the laser. The temporal bubble dynamics - growth, collapse, rebound and associated flow characteristics of high speed re-entrant jet and high pressure waves were modelled as a function of bubble stand-off distance. Results were compared to published research. The model successfully computes bubble formation and collapse dynamics, re-entrant jet structure and magnitude, the associated pressure field, and sensitivity to stand-off distance.

Introduction

Cavitation bubbles form in liquid when the pressure of the liquid drops below the saturated vapour pressure, this causes a bubble to form, expand and quickly collapse resulting in the emission of a high pressure pulse [4]. When vapour cavities become entrained by the flow they can collapse near solid boundaries, causing surface damage [7]. Cavitation damage affects various turbomachinery and hydraulic equipment, including impeller blades, valves and ship propeller blades [3]. Depending on the design of the machine and the duration and extent of the exposure to cavitating flows, cavitation can affect the performance of the machine and lead to unwanted noise and vibration issues [2].

A complete understanding of the dynamics of single bubble formation and collapse is essential to the development of a computational model that could predict cavitation erosion. A significant amount of experimental research has been performed examining the formation and collapse of a single bubble through various means, the most common of which are spark generation, laser generation or acoustic generation [15]. A single bubble is often generated near a solid boundary in order to observe the effect the collapse of the bubble has on a solid surface [1,3,5,11,15,17,18]. High-speed photography and advanced optical techniques have shown that when a bubble collapses near a surface a large localized shock wave is emitted and a high-speed jet travels towards the surface [15]. The debate over which

of these phenomena is primarily responsible for cavitation damage is a long one; however, both phenomena are indicative of bubble collapse.

One of the most common experimental methods for generating a single bubble is through the use of a laser. Typically an optical system focuses the energy from the laser into a small focal volume, causing a local heating of the water that is dependent on the energy of the laser beam, the type of laser used, the focusing angle and the laser pulse duration [19]. A Nd:YAG laser is often used [1,5,15], which depending on the laser can have pulse durations between nanoseconds and femtoseconds [19]. The entire formation and collapse process occurs on a very small scale; a cavitation bubble typically has a maximum radius on the order of 1 mm and a collapse time on the order of 100 microseconds [4]. Despite the small size of the bubble and the short duration of the collapse, the pressures generated by the bubble are very large, approximately on the order of 100 MPa [15]. It is the extreme discrepancies between these scales that has complicated the study of cavitation erosion.

It has been experimentally determined that the standoff distance, the ratio of the distance between the center of the bubble at formation and the solid surface and the maximum radius of the bubble, is an important parameter that affects not only the damage pattern but also the magnitude of the pressure and velocity fields at collapse [1,5,15,17]. At close standoff distances a large amount of damage is observed [15], which is due to the contact between the bubble wall and the solid surface during collapse [5]. Significant damage is also seen at other standoff distances, which could be due to the magnitude of the shock wave, the high-speed microjet or the effect of surface tension.

Modeling the collapse of a single bubble has been accomplished using simplified methods such as the Rayleigh-Plesset equation and the Boundary Integral Method, as well as more complex methods such as CFD. Johnsen and Colonius modeled the collapse of a non-spherical bubble using a compressible two-phase homogeneous CFD model; examining both Rayleigh collapse and shock induced collapse [9]. Müller et al. used experimental data from laser-generated bubble collapse to estimate conditions at the maximum radius of the bubble formation and initialize the CFD solution of the collapse of a laser-generated bubble using a homogeneous compressible, two-phase flow method [14]. Zein et al. used a compressible two-phase non-equilibrium model to simulate the phase transition of a laser-generated cavitation bubble, including the heat and mass transfer between the two phases [21].

Akhatov et al. used a mathematical model to simulate the collapse of a laser-generated bubble which included the effects of the compressibility of the liquid, the heat and mass transfer between the phases, and the evaporation and condensation of the fluid at the bubble wall [1]. Dreyer et al. also took an analytical

approach and created a set of ordinary differential equations that could be solved using the Runge-Kutta methods under different assumptions to model laser-generated cavitation bubbles [6]. Zein [20] and Dreyer et al. [6] both concluded that including a phase change model was necessary to capture the temperature difference between the two phases, while the assumption that the bubble initially contains a small amount of non-condensable gas was essential for creating a rebound bubble whose shape matched the experimental data of Müller et al. [14]. Although a phase change model is important for accurately modeling the temperature distribution of a laser-generated cavitation bubble, it has been found to not have a significant effect on the evolution of the bubble radius [6]. Whether it has a prominent effect on the pressure and velocity fields of the collapse of a single laser-generated bubble remains to be determined.

In this paper we will examine the physics of laser-generated bubble collapse using a compressible multi-phase pressure-based solver developed for the open source CFD tool OpenFOAM by Müller et al. [13]. The CFD solution of the collapse of a laser-generated bubble in a free field will be compared to both the Rayleigh-Plesset equation as well as experimental data. The CFD solutions of bubble collapse near a solid surface will also be examined, using the standoff distance as the primary parameter to determine the influence of the distance to the wall on the dynamics of bubble collapse. A separate, thermal analysis was also conducted using OpenFOAM to model the temperature field generated by a Nd:YAG laser when forming a cavitation bubble.

Governing Equations

Thermal Analysis

A computational analysis of the heat diffusion from a ND-Yag laser pulse was performed using the energy equation with a source term that accounts for the physics of the laser process and its effect on the temperature distribution of the water. This source term, A , is dependent on the maximum laser intensity, the reflectivity, the absorption coefficient of the water at a specific wavelength and the normalized spatial and temporal profiles of the laser pulse [8]. For a laser with a Gaussian intensity profile and a triangular-shaped temporal profile, the energy equation with the inclusion of the source term can be written as follows [12,16].

$$\rho c_p \frac{\partial T}{\partial t} = k \nabla^2 T + A \quad (1)$$

$$A = \frac{2P}{\pi w^2} (1 - R_w) a_w e^{-a_w x} e^{-2\left(\frac{r}{w}\right)^2} \frac{t}{a} \text{ for } 0 \leq t \leq a \quad (2)$$

$$A = \frac{2P}{\pi w^2} (1 - R_w) a_w e^{-a_w x} e^{-2\left(\frac{r}{w}\right)^2} \frac{2a - t}{a} \text{ for } a \leq t \leq 2a \quad (3)$$

In equations (2) and (3) P is the laser power, w is the radius of the beam, t is the time and a is the rise time of the peak laser intensity. There are two constant coefficients in the source term, the reflectivity R_w and the absorption coefficient a_w , both of which are dependent in this case on the wavelength of the laser and the medium being penetrated by the laser beam.

Compressible Multiphase Analysis

The compressible multi-phase pressure-based solver used in this research is a homogeneous flow model developed by Miller et al. [13]. In a homogeneous flow model the conservation equations reduce to a single mass equation and a single momentum equation, given by equation (4) and equation (5) [13].

$$\frac{\partial \rho}{\partial t} + \nabla \cdot (\rho \mathbf{u}) = 0 \quad (4)$$

$$\frac{\partial}{\partial t} (\rho \mathbf{u}) + \text{div}(\rho \mathbf{u} \otimes \mathbf{u}) - (\text{grad } \mathbf{u}) \text{grad } \mu_{\text{eff}} - \mu_{\text{eff}} \Delta \mathbf{u} = -\text{grad } p_d - (\text{grad } \rho) \mathbf{g} \cdot \mathbf{x} \quad (5)$$

The density will be different for each phase, a mixture density is calculated which is determined based on the volume fraction of each phase and the density of each phase [13].

$$\rho = \alpha_1 \rho_1 + \alpha_2 \rho_2 \quad (6)$$

The volume fraction is an indicator of the ratio of the phases at any point in the flow, the sum of the volume fraction must be one, as seen in equation (7).

$$\alpha_1 + \alpha_2 = 1 \quad (7)$$

Two additional equations of state are also needed. The equation of state for the gas phase is based on the assumption that the vapor inside of the bubble behaves as an ideal gas and only undergoes isentropic processes [13].

$$\rho = \left(\frac{p}{a_c} \right)^{\frac{1}{\kappa}} \quad (8)$$

The equation of state for the liquid phase is derived from the speed of sound in a medium, assuming that the sound speed is constant and the process is isentropic [13].

$$\rho = \rho_0 + \frac{1}{c^2} (p - p_0) \quad (9)$$

From these governing equations momentum, pressure and volume fraction equations are derived. The equations were then linearized and the complete set of equations solved using a cell-centered, co-located finite volume method [13]. Miller et al. [13] provides a more detailed description of the implementation of the method, discretization of the governing equations and a detailed description of the solution algorithm.

Modelling efforts were performed using OpenFOAM an open source CFD flow solver. Laser heating modelling was performed using a modified version of the scalarTransportFoam solver with temperature as the transported scalar. Bubble collapse modelling was performed using a compressible, multi-phase, homogenous pressure based OpenFOAM finite volume solver created to model underwater explosions by Miller [13]. Christian [22] provides a detailed discussion of the OpenFOAM modelling efforts.

Results

CFD of Laser Heating

The numerical modeling of the laser induced cavitation bubble formation was accomplished by modeling a Nd:YAG laser with characteristics summarized in Table 1. The reflectivity (R_w) and absorption coefficient (a_w) are both dependent on the medium as well as the wavelength of the laser. R_w is a unitless coefficient that has a value of 0.012 for a 530 nm laser in water [23]. The direction along the beam (and wall for the wall bounded study) is X. The Y direction is orthogonal to X. The bubble center is initiated at X=0 and Y is defined by the standoff distance in the wall bounded study.

a_w for tap water is harder to accurately determine. Literature suggests for pure water at a wavelength of 532 nm a_w ranges between 0.04 - 0.05 1/m [23]. However, a_w for tap water is usually much higher and is a function of particulate concentration. Furthermore, a_w increases during laser-induced water vaporization leading to plasma formation [24].

Laser Power (MW), E_p	3
Beam Waist (μm), w_0	3.765
Reflectivity, R_w	0.012
Absorption coefficient (1/m), a_w	5
Laser rise time (ns), a	5
Rayleigh length (μm), z_0	83.7
Focal length (m), L	0.15
Wavelength of laser (μm), λ	532
Thermal diffusivity (m^2/s), k	1.43×10^{-7}
Density (kg/m^3), ρ	998
Specific heat capacity ($\text{J}/\text{kg}\cdot\text{K}$), c_p	4180

Table 1: Laser and fluid parameters for CFD of laser heating

Experiments were performed to measure a_w as a function of particulate concentration and values ranged from 0.9 to 37 1/m for distilled H_2O to up to 0.2% particulate concentration by volume. For this study, a_w was chosen to be 5 1/m. Figure 1 is a contour plot of the water temperature at the end of the laser pulse (time=10ns). The results indicate that local temperatures are sufficient to vaporize water.

CFD of Single Bubble Collapse in a Free Field

Modeling the collapse of a single bubble in a free field was used as a test case to verify the CFD model with comparison to

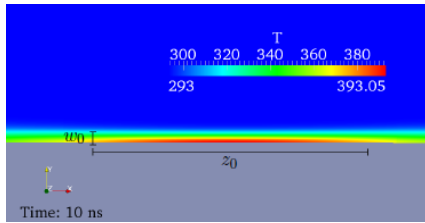


Figure 1. Contour of water temperature at end of laser pulse.

predictions from the Rayleigh-Plesset equation and from the experiments of Müller et al. [14]. Figure 2 shows the growth and collapse of a bubble as a function of time. The Rayleigh-Plesset equation is only valid for the initial bubble formation and collapse. Good agreement is observed between the CFD solution and Müller [14] for the initial formation and collapse of the bubble, including the maximum radius and the collapse time. However, the size of the rebound bubble is noticeably over predicted by the CFD solution. Adding a phase change model that could account for the evaporation and condensation across the interface of the two phases, as well as model the heat transfer resulting from the temperature rise, could result in a CFD model that would more accurately model the rebound bubble. Zein [20] and Dreyer et al. [6] found that the best correlation between the results of their models and the experimental data of Muller et al. [14] occurred when they accounted for phase change.

CFD of Single Bubble Collapse Against a Wall

The collapse of a single cavitation bubble adjacent to a solid wall was investigated using the same initial conditions as the free

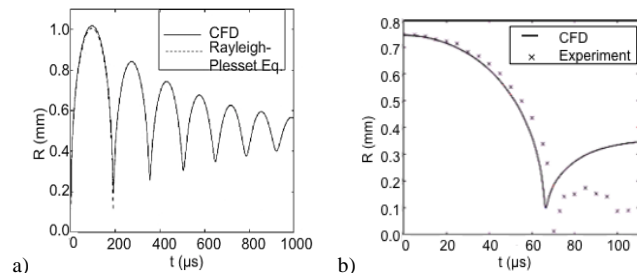


Figure 2. Bubble radius vs Time. a) comparison to Rayleigh-Plesset. b) comparison to Muller [14] – $P_{G0}=4.579$ Pa & $R_0=R_{\text{max}}=746.9\mu\text{m}$.

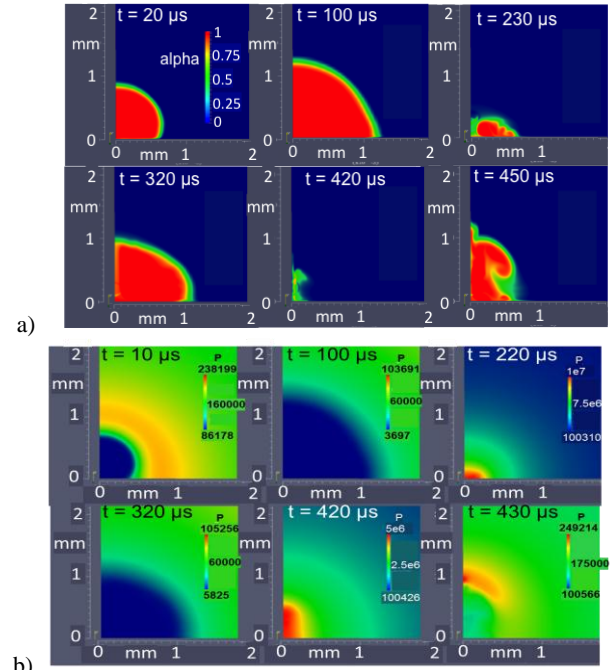


Figure 3. Volume fraction and pressure for $\gamma = 0.2$ at different times in the bubble formation and collapse.

bubble case. Different standoff distances ($\gamma = s/R_{\text{max}} \equiv$ bubble center to wall distance / max radius) were examined ($\gamma = 0.2, 0.5, 0.7, 1.0$ and 1.3). Trends were compared with the literature for cavitation bubble collapse [1,15, 17-19]. Qualitatively, the effect of γ on the modeled pressure and velocity fields agree with published data.

The dynamics of bubble collapse are similar for each standoff distance; the initial high pressure inside of the bubble causes it to expand until the bubble reaches its maximum size. The bubble then rapidly collapses, upon collapse a high pressure pulse is emitted and a microjet travels from the center of the bubble to the wall. The bubble then expands a second time, this time with a much smaller maximum radius, and collapses a second time, leading to yet another high pressure pulse. Phillip et al. [15] found that the most damage was produced to a solid surface for $\gamma \leq 0.3$ and $1.2 \leq \gamma \leq 1.4$. Figure 3 shows the computed bubble volume fraction and pressure field for the $\gamma = 0.2$ case.

Figure 4 shows the wall pressure and velocity magnitude for $\gamma = 0.2$. High wall pressure is observed during the first bubble collapse and with high velocities in the micro jet. At $\gamma = 1.0$, bubble ‘‘Splash’’ was observed in the simulations in agreement with Brujan et al [5] where the microjet travels through the bubble during collapse and interacts with the collapse induced flow field generating a ‘‘Splash’’ effect on the wall.

Figure 5 shows the max wall pressure, velocity and wall-shear as a function of γ . The data show good agreement with results of [15] for velocity magnitude and [23] for wall shear. While [15] observed jet impact velocity decreased with increasing γ , these results show the velocity magnitude increasing with γ . Review of

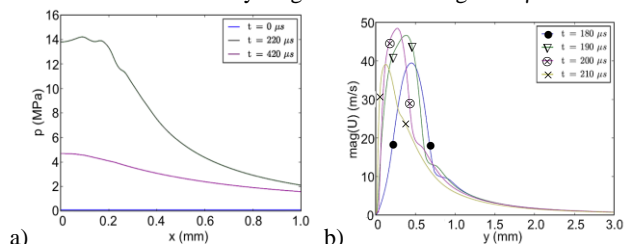


Figure 4. Wall pressure magnitude and velocity magnitude for $\gamma = 0.2$. a) Pressure vs X, b) velocity magnitude vs Y at X=0.

the velocity profile near the wall for the larger γ suggests that the profile shifts in Y exhibiting a broader profile with lower velocity at a given Y. This trend may explain the trend observed by [15] although it is unknown what distance from the wall velocities were measured.

Conclusions

The formation and collapse of a laser-generated cavitation bubble was modeled computationally using OpenFOAM. A compressible flow model was used to compute pressure and velocity fields of a growing and collapsing bubble. The energy equation was solved separately to compute the temperature distribution for the formation of a single laser-generated cavitation bubble. After successfully modeling the heating by pulsed laser and the collapse of a bubble near a wall, future work will focus on coupling the CFD models to simulate the complete formation and collapse of a laser-generated cavitation bubble. This computational effort would solve the three conservation equations simultaneously with a phase change model for micro-scale evaporation with increasing temperature as a laser generated bubble forms. Although the computational results discussed in this work relied on a CFD method that only solved the mass and momentum equations, the complex dynamics of bubble collapse against a wall appear to be captured using a homogeneous multiphase compressible finite volume method.

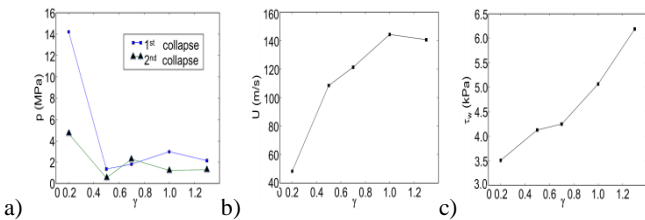


Figure 5. a) Max wall pressure at first and second collapse, b) max velocity magnitude and c) wall shear stress as a function of γ .

Acknowledgments

This research is supported by the Dept of Energy (DoE) and Sandia National Laboratories (SNL) through cont. # 775396 & 2012-6823C. SNL is a multi-program lab managed and operated by Sandia Corp, a wholly owned subsidiary of Lockheed Martin Corporation, for the U.S. DoE Nat. Nuclear Security Administration under contract DE-AC04-AL85000. The project and technical managers are Matthew Barone and Erick Johnson.

References

- [1] Akhatov, I., Lindau, O., Topolnikov, A., Mettin, R., Vakhitova, N., & Lauterborn, W., Collapse and rebound of a laser-generated cavitation bubble, *Phys. Fluids*, **13**, 2805, 2001.
- [2] Arndt, R., Cavitation in fluid machinery and hydraulic structures, *Ann. Rev. of Fluid Mechs.*, **13**, 1981, 273-326.
- [3] Blake, J. & Gibson, D., Cavitation bubbles near boundaries, *Ann. Rev. of Fluid Mechs*, **19**, 1987, 99-123.
- [4] Brennan, C., *Cavitation and Bubble Dynamics*, Oxford University Press, 1995.
- [5] Brujan, E., Keen, G., Vogel, A. & Blake, J., The final stage of the collapse of a cavitation bubble close to a rigid boundary, *Phys. of Fluids*, **14**, 2002, 85.
- [6] Dreyer, W., Duderstadt, F., Hantke, M. & Wanecke, G., Bubbles in liquids with phase transition, *Continuum Mechs. and Thermodyn.*, 2011, 1-23.
- [7] Franc, J.P. & Michel J.M., *Fundamentals of cavitation*, Kluwer Academic Publ., 2004.
- [8] Hicks, J., Urbach, L., Plummer, E., & Dai, H., Can pulsed laser excitation of surfaces be described by a thermal model?, *Physical review letters*, **61**, 1988, 2588-2591.
- [9] Johnsen, E. & Colonius, T., Numerical simulations of non-spherical bubble collapse, *J. Fluid Mech*, **629**, 2009, 231-262.
- [10] Koivula, T., On cavitation in fluid power, *Proc. of 1st FPNI-PhD Symp. Hamburg*, 2000, 372-382.
- [11] Lauterborn, W. & Bolle, H., Experimental investigations of cavitation bubble collapse in the neighbourhood of a solid boundary, *J. Fluid Mech*, **72**, 1975, 391-399.
- [12] Lin, J. & George, T., Laser-generated electron emission from surfaces: Effect of the pulse shape on temperature and transient phenomena, *J. of App. Phys.*, **54**, 1983, 382-387.
- [13] S.T. Miller, D.A. Boger, H. Jasak, and E.G. Paterson. "A compressible pressure-based finite-volume method for homogeneous two-phase mixtures including multiple gas species." Int Conf on Num Meth for Multiphase Flows, State College, PA; June, 2012.
- [14] Müller, S., Bachmann, M., Kröninger, D., Kurz, T. & Helluy, P., Comparison and validation of compressible flow simulations of laser-induced cavitation bubbles, *Comps & Fluids*, **38**, 2009, 1850-1862.
- [15] Philipp, A. & Lauterborn, W., Cavitation erosion by single laser-produced bubbles, *J of Fluid Mech*, **361**, 1998, 75-116.
- [16] Shen, W., Zhang, J., & Yang, F., Three-dimensional model on thermal response of skin subject to laser heating, *Comp. Meth. in Biomechs and Biomed Eng.*, **8**, 2005, 115-125.
- [17] Tomita, Y. & Shima, A., Mechanisms of impulsive pressure generation and damage pit formation by bubble collapse, *J. Fluid Mech*, **169**, 1986, 535-564.
- [18] Vogel, A., Lauterborn, W. & Timm, R., Optical and acoustic investigations of the dynamics of laser-produced cavitation bubbles near a solid boundary, *J. Fluid Mech*, **206**, 1989, 299-338.
- [19] Vogel, A., Noack, J., Nahen, K., Theisen, D. Busch, S. Parlitz, U., Hammer, D., Noojin, G., Rockwell, B. & Birngruber, R., Energy balance of optical breakdown in water at nanosecond to femtosecond time scales, *App. Phys. B: Lasers and Optics*, **68**, 1999, 271-280.
- [20] Zein, A., *Numerical methods for multiphase mixture conservation laws with phase transition*, Ph.D. thesis, Otto-von-Guericke-Universität Magdeburg, Universitätsbibliothek, 2010.
- [21] Zein, A., Hantke, M. & Warnecke, G., Modeling phase transition for compressible two-phase flows applied to metastable liquids, *J. Comp. Physics*, **229**, 2964-2998.
- [22] Christian, C.M., "Modeling Laser-Generated Cavitation Bubbles," MS Thesis, Mech. Eng., Penn State Univ., 2012.
- [23] Dijkink, R. and C. Ohl, "Measurement of cavitation induced wall shear stress," *Appl. Phys. Let.*, 93(25), pp. 254107-254107, 2008.